

Development of a new method to measure surface tension of molten oxides

TOSHIKI KONDO, HIROAKI MUTA AND YUJI OHISHI*

*Graduate School of Engineering, Osaka University,
Yamadaoka 2-1, Suita, Osaka, Japan*

Received: August 22, 2019. Accepted: October 21, 2019.

Physical properties of molten oxides such as viscosity and surface tension are important in various fields. However, it is very difficult to measure the properties of molten oxides owing to their high melting points, high reactivity, and high vapor pressure. Hence, the physical properties of molten oxides are scarcely reported. Therefore, we developed a new method, termed the “impingement method,” for measuring the surface tension of molten oxides in a very short time, using the aerodynamic levitation technique. In this work, we developed an apparatus for measuring the surface tension of molten Al_2O_3 and compared the value with that of other methods, considered as reference values. Results showed that the surface tension of molten Al_2O_3 was approximately 0.72 N/m at around 2500 K, which is close to the reference value; moreover, the measurements could be obtained in a very short time (approximately 80 ms). Thus, it is expected that the surface tension of molten materials with high vapor pressures such as ZrO_2 and UO_2 can be measured using this method.

Keywords: Al_2O_3 , liquid phase, surface tension, aerodynamic levitation, molten oxide

1 INTRODUCTION

Physical properties such as viscosity and surface tension of molten oxides such as Al_2O_3 and ZrO_2 have attracted significant attention in various fields where high-temperature operation is required, such as aerospace engineering [1], material science [2], and nuclear engineering [3]; as these oxides are

*Corresponding author: ohishi@see.eng.osaka-u.ac.jp

widely used as refractory materials owing to their high melting point. In addition, in the nuclear engineering field, much attention has been paid to molten oxides containing U, Zr, and Fe in the wake of the core-meltdown accident at Japan's Fukushima-Daiichi nuclear power plant in 2011 as they are the components of the reactor cores. The physical properties of the molten core materials are expected to allow the prediction of the convection, dropping, and spreading behavior of the melts. The common property of these oxides is that they have high melting points, which makes measurement significantly difficult.

As for the viscosity measurements, Langstaff *et al.* proposed a new method to measure the viscosity of oxides based on the aerodynamic levitation (ADL) technique, which is one of the contactless methods [4]. In this technique, a droplet is levitated via ADL and oscillated using speakers. The viscosity is evaluated from the damping behavior during oscillation. They demonstrated that the viscosity of Al_2O_3 could be evaluated successfully by this technique. Very recently, our group showed that this technique can be adapted to an oxide with a much higher melting point, namely ZrO_2 [5].

In contrast, the surface tension measurement of oxides had been a difficult challenge. For the past few decades, surface tension of molten Al_2O_3 has been evaluated using the sessile drop [6] and maximum bubble pressure methods [7]. However, these conventional methods are not reliable at extremely high temperatures because the sample's surfaces would be contaminated by the reaction between the samples and the container during the measurements [8]. Recently, Langstaff *et al.* successfully measured the surface tension of Al_2O_3 at 2523 K [4]; they used ADL and thus avoided this difficulty. They induced oscillation using speakers, found five resonance modes by scanning frequency, and evaluated the surface tension from the resonance frequencies using the sum rule [9]. The resultant surface tension was higher than those measured by the sessile drop and maximum bubble pressure methods by more than 20%, suggesting that conventional techniques are not appropriate for high-temperature melts.

Although the abovementioned ADL-based technique provides reliable surface tension measurements, it is not realistic to use this technique to measure temperature-dependent surface tension; moreover, it is not feasible to adapt this technique to oxide melts other than Al_2O_3 as this technique requires considerably long measurement times (about few minutes) and much effort to find all of the five resonance modes by scanning frequency. This is supported by the fact that Langstaff *et al.* reported the surface tension of Al_2O_3 at only one temperature (2523 K) [4]. The long measurement time also causes difficulties in surface tension measurements of evaporative substances. As the resonance frequency depends not only on the surface tension but also on the volume of the droplet, evaporation of the sample will change the resonance frequencies, which makes the measurement significantly difficult. This means that the technique proposed by Langstaff *et al.* cannot be adapted to

evaporative oxides such as ZrO_2 and UO_2 (the vapor pressures of Al_2O_3 , ZrO_2 , and UO_2 at each melting temperature are 0.12 Pa, 18 Pa, and 3100 Pa, respectively based on the FACT53 [10] thermodynamic database). To measure the surface tension of high-temperature evaporative oxide melts, it is necessary to develop a new method that facilitates measurement in a short duration.

Therefore, the objective of this study was to develop a new method to measure the surface tension of molten oxides within one second. We named this technique as the “impingement method”. A schematic describing the principle of this method is shown in Fig. 1. In this method, the surface tension is evaluated from the impingement behavior of a droplet. First, the droplet is levitated using a levitation technique. The droplet is then dropped onto a ceramic plate so that it impinges on the plate. Just before impingement, the droplet has a certain amount of kinetic energy. When the droplet does not wet the substrate, the droplet keeps deforming during impingement until all of the initial kinetic energy is transformed into surface energy except for the energy lost because of viscosity. As the surface energy is a function of the surface area and surface tension, the surface tension can be calculated from the initial kinetic energy, surface area, and viscous dissipation. In our study, we demonstrated that this impingement method enables surface tension measurements of Al_2O_3 within one second.

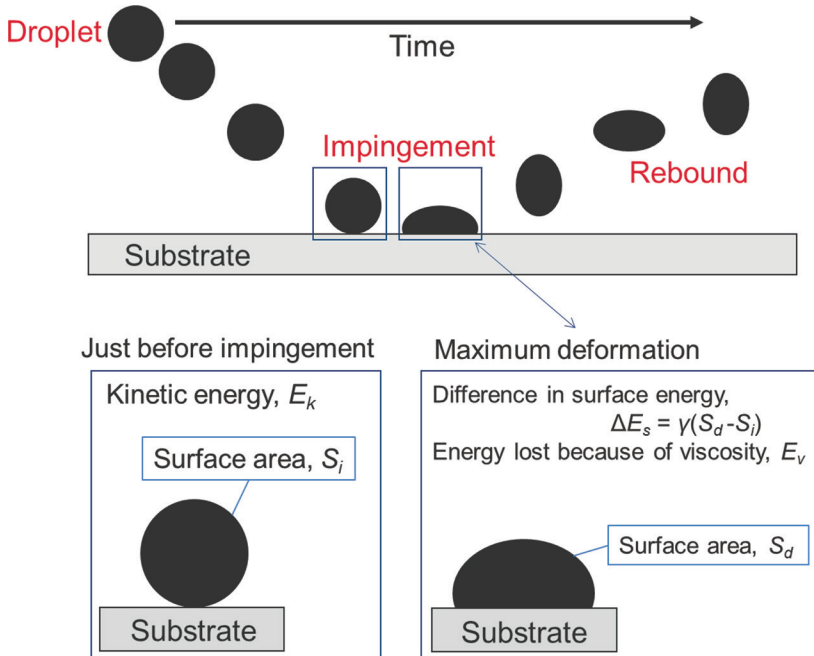


FIGURE 1
Concept of the droplet impingement method.

2 EXPERIMENTAL

Figure 2(a) is the schematic of the measurement system, and figure 2(b) shows the diagram of the apparatus. The levitation system consists of a separable conical converging–diverging nozzle (diameter of the converging part is 1 mm) driven by gas pressure, and a levitation gas supplying system. A gas mixture comprising approximately 15% O₂ and 85% Ar gases was supplied to the nozzle using a mass flow controller at a typical combined flow rate of 400 cm³ min⁻¹. O₂ was added to prevent the reduction of samples during the experiments. First, the sample was levitated using the closed nozzle by supplying levitation gas; the sample was melted by a 100-W CO₂ laser (Coherent, GEM100) emitted at a wavelength of 10.6 μm. The nozzle was

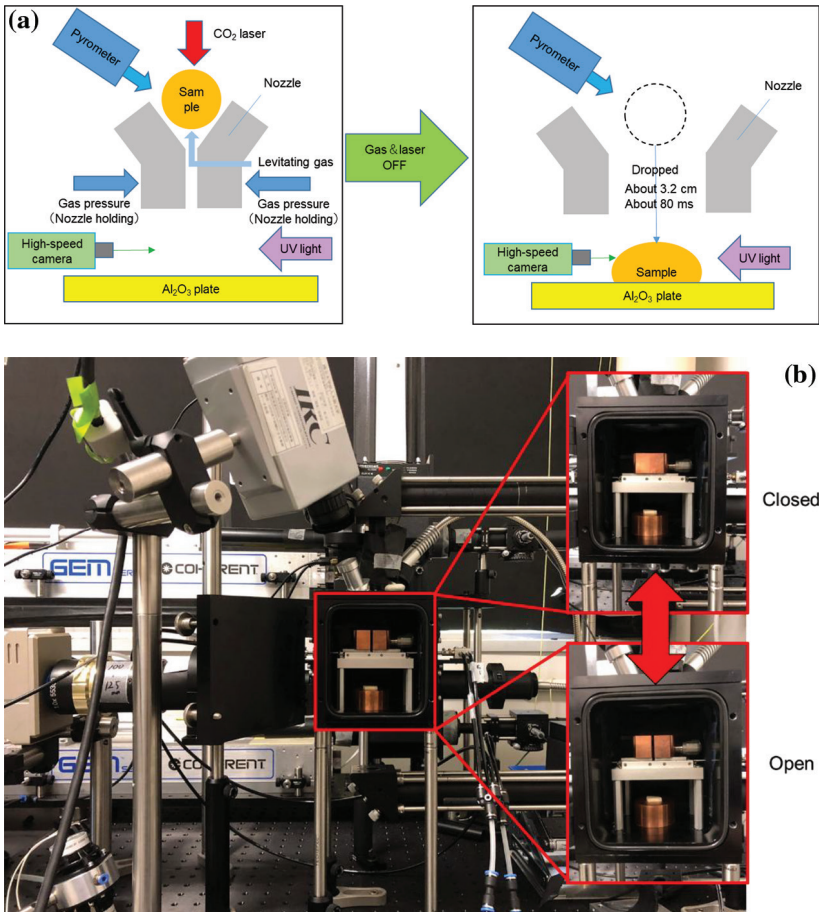


FIGURE 2
 (a) Schematic of the impingement analysis system; (b) Diagram of the impingement analysis system.

then opened to drop the sample onto the ceramic plate, placed approximately 3.5 cm below the nozzle. It takes approximately 80 ms for the sample to fall and impinge the plate if air resistance is ignored. The impingement behavior of the Al_2O_3 sample with respect to the plate was observed using a 2000-fps high-speed camera (Ditect, HAS-D72M) equipped with a telecentric lens (Edmund, TS GOLD). We used ultraviolet (UV) light as the back light (Hamamatsu, Ls9588-02A) with a 370 ± 2 nm bandpass filter. The images were analyzed using the original tool (Ditect, Deep macro II) to determine the center of gravity of the sample, that of the edge of the sample, and the length of the edge of the sample. A 2-mm diameter stainless used steel ball was used for length calibration.

The surface tension was evaluated from the deformation of the droplet during impingement, as shown in Fig. 1. For simplicity, we assumed the droplet to be a true sphere before impingement, and that there was no interaction between the droplet and substrate. We focused on two points of time: just before impingement and the time when the velocity of the droplet became zero. Just before impingement, the droplet has a certain amount of kinetic energy, E_k . During impingement, the droplet deforms; therefore, part of the initial kinetic energy is converted to surface energy because of the increasing surface area and to heat via viscous deformation. When the velocity of the droplet becomes zero, all of the initial kinetic energy is converted to surface energy except for the energy lost because of viscosity, implying maximum deformation. By comparing the energies of these two points of time, the following relationship was derived using the energy conservation law:

$$E_k = \Delta E_s + E_v, \quad (1)$$

where E_s is the surface energy and E_v is the energy lost via viscous deformation. ΔE_s is the increased surface energy because of deformation. The increased surface energy ΔE_s is described elsewhere [11].

$$\Delta E_s = \gamma(S_d - S_i) \quad (2)$$

where S_i is the surface area before impingement and S_d is the surface area of the deformed sample. These equations indicate that the surface tension can be calculated by determining E_k , S_d , S_i , and E_v .

The kinetic energy and surface areas, E_k , S_d , and S_i , were determined from the recorded images. Figure 3 (a) shows the images of the Al_2O_3 sample impinging the substrate. It should be noted that the edge of the sample is clearly recorded. To derive E_k , S_d , and S_i , the recorded images were binarized, as shown in Figs. 3 (b). E_k was determined from adjacent images taken just before impingement (in this case, 0 and 0.5 ms). The distance of the center of the gravity of the sample between these two images (a) was calculated, which is the distance moved during one frame (0.5 ms) just before the impingement. Then, E_k was calculated as

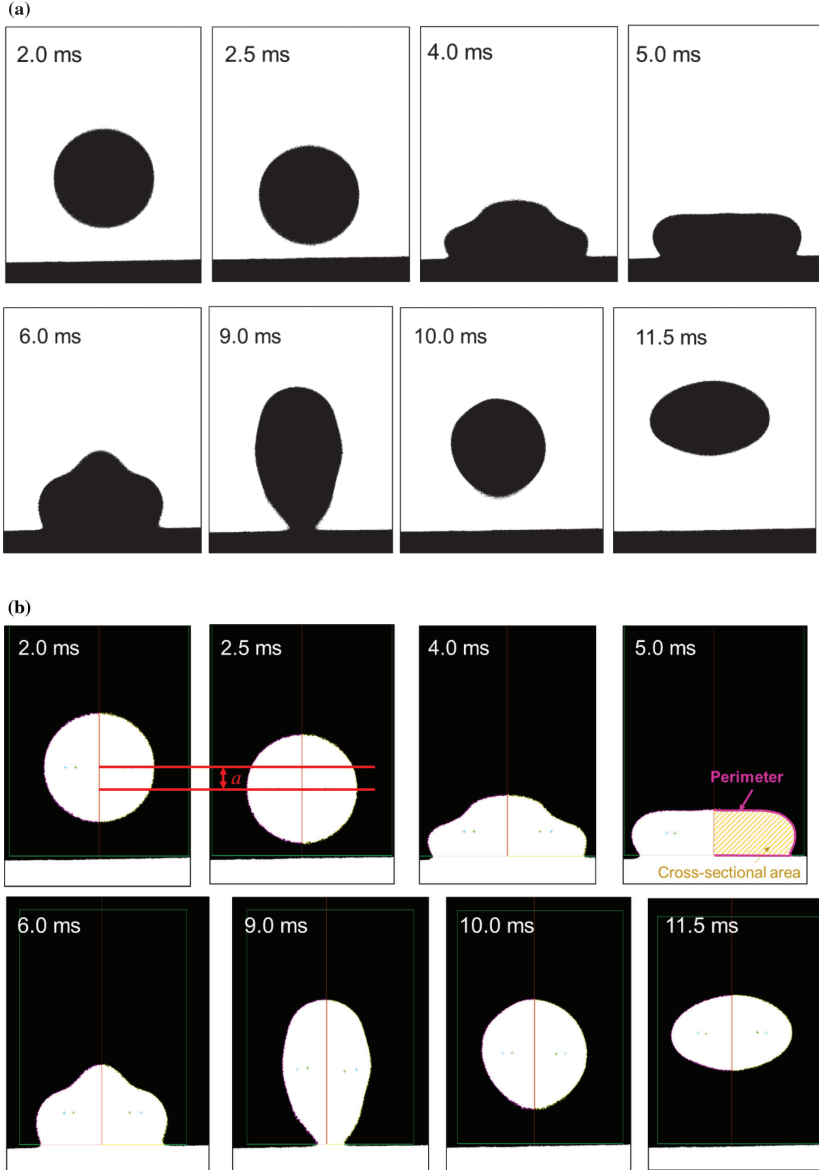


FIGURE 3

(a) Images of the sample during impingement; (b) Images of the analyzed sample.

$$E_k = \frac{1}{2} m \left(\frac{a}{0.5} \right)^2, \quad (3)$$

where m is the mass of the sample measured after the experiment.

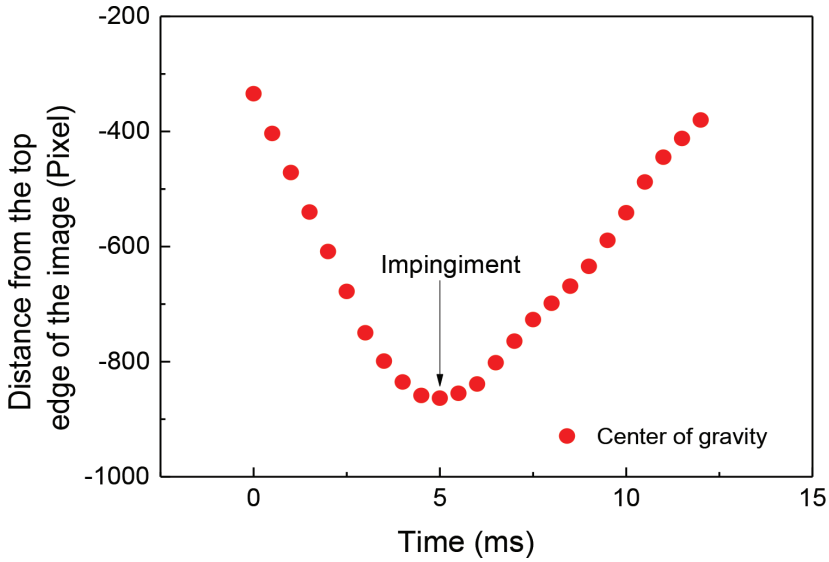


FIGURE 4
Time dependence of the center of gravity of the sample.

As S_d was determined from the image obtained when the kinetic energy of the sample became zero, the z position of the center of gravity was plotted as a function of time, as shown in Fig. 4 (in this case, 5 ms). The image taken at the time when the center of gravity became minimum was used for deriving S_d . S_d was calculated from the perimeter using the Pappus–Guldinus equation with the z axis being rotationally symmetric [12]. S_i was estimated as the surface area of a true sphere with the same volume as the deformed sample, which was calculated from the cross-sectional area of the sample using the Pappus–Guldinus equation [12].

The energy lost because of viscous deformation of the sample during impingement, E_v , was calculated by assuming the deformation from the initial spherical shape to the maximum deformation to be equal to that during 1/4 the period of the well-known damped oscillation. The lost energy during 1/4 the period of the damped oscillation is given as [13]

$$E_v = \pi\zeta E_m, \quad (4)$$

$$\Gamma T_o = \frac{2\pi\zeta}{\sqrt{1-\zeta^2}}, \text{ and} \quad (5)$$

$$\Gamma = \frac{5}{\rho R^2} \eta, \quad (6)$$

where Γ is the damping oscillation constant, T_o is the time for a period of oscillation, ζ is the energy reduction rate, ρ is the density of the material [4], and R is the radius of the sample when it is regarded as the spherical shape. Γ could be calculated from the viscosity of the sample, which was taken from the literature [4]. The time between the sample contacting the plate and the maximum deformation was evaluated from the recorded image of the sample and found to be 2.0 ms for all the cases. Thus, E_v was calculated using Eqs. (4), (5), and (6) by considering T_o as 8 ms.

The temperature of the sample during impingement was estimated from the free cooling behavior of the sample measured prior to the dropping experiment and the free-fall time of the sample. The sample was levitated via ADL and melted using the heating laser. The temperature was measured using a single-color (0.9 μm) pyrometer (Chino, IR-CAS8CNL). The data were recorded every 2 ms by a data logger (Graphtec, GL-900). The heating laser was turned off without opening the nozzle to obtain the cooling curve. A typical example of the cooling curve obtained from molten Al_2O_3 is shown in Fig. 5. In this case, the laser was turned off at 140 ms, and solidification started at 890 ms. Once the solidification starts, the temperature remains constant until the liquid area disappears. The temperature (T) of the samples was estimated from the temperature measured by the pyrometer (T_p) using Wien's law as follows [14]:

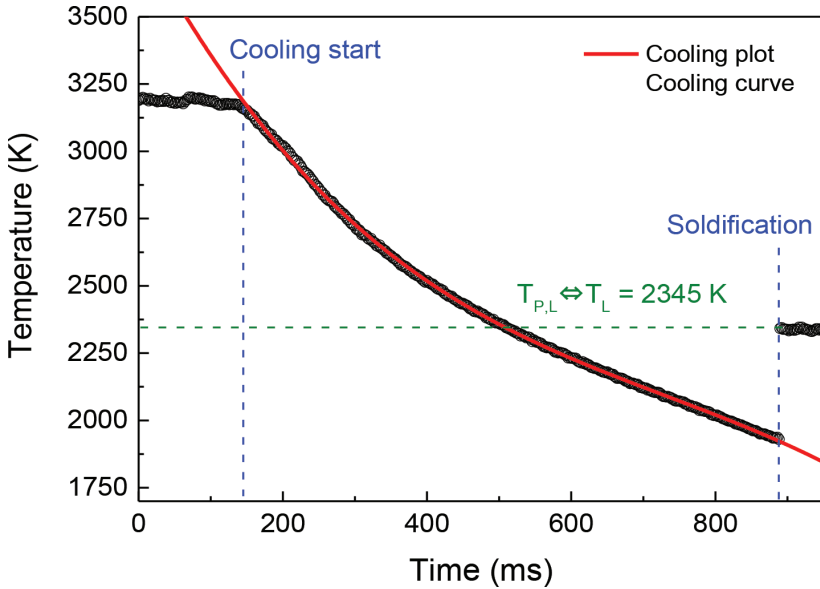


FIGURE 5
Cooling curve for the sample.

$$\frac{1}{T} - \frac{1}{T_p} = \frac{1}{T_L} - \frac{1}{T_{L,p}}, \quad (7)$$

where T_L is the melting point and $T_{L,p}$ is the melting point measured by the pyrometer; all temperatures are in Kelvin. The value of T_L used for liquid Al_2O_3 was 2345 K [15], and that of $T_{L,p}$ was determined based on the cooling curve. We applied this equation assuming that the emissivity of the sample does not change in the temperature range of interest.

The cooling curve was fitted using a polynomial formula given by

$$T = At + Bt^2 + Ct^3 + Dt^4, \quad (8)$$

where A, B, C, and D are the fitting parameters, and t is the time. Assuming the cooling rate to be almost identical between the levitated sample and dropped sample, the sample temperature during impingement was estimated by including the free-fall time of the sample for t in this equation. The free-fall time was calculated from the speed of the sample just before impingement. The calculated free-fall time was approximately 84 ms, which is almost the same as the theoretical free-fall time calculated based on the distance between the nozzle and substrate by ignoring the air resistance.

3 RESULTS AND DISCUSSION

3.1 Measurement results

Figure 6 presents the results of the surface tension measurements along with the reference data. Reference data were recorded via the droplet oscillation method using ADL [4], droplet rotating method using ADL [16], sessile drop method [6], and maximum bubble pressure method [7]. The data obtained using the droplet oscillation method [4] were divided into two groups: the ones calculated using the sum rule from all of the split resonance frequencies and those calculated only from the frequency of the mode with $l = 2$ and $m = 0$. As mentioned in the introduction, the values obtained using the sum rule were considered to be the most reliable ones, which are roughly 20% higher than the other reported values. Our results were almost identical to that obtained through the oscillation droplet method using the sum rule, indicating that our method could provide reliable surface tension measurements.

Our results show that the surface tension of Al_2O_3 is almost independent of temperature; this is reasonable as it is known that surface tensions of several liquids are almost constant or decrease slightly with increasing temperatures [8]. The temperature dependence of the surface tension measured using our method was considerably close to that measured using the droplet oscillation

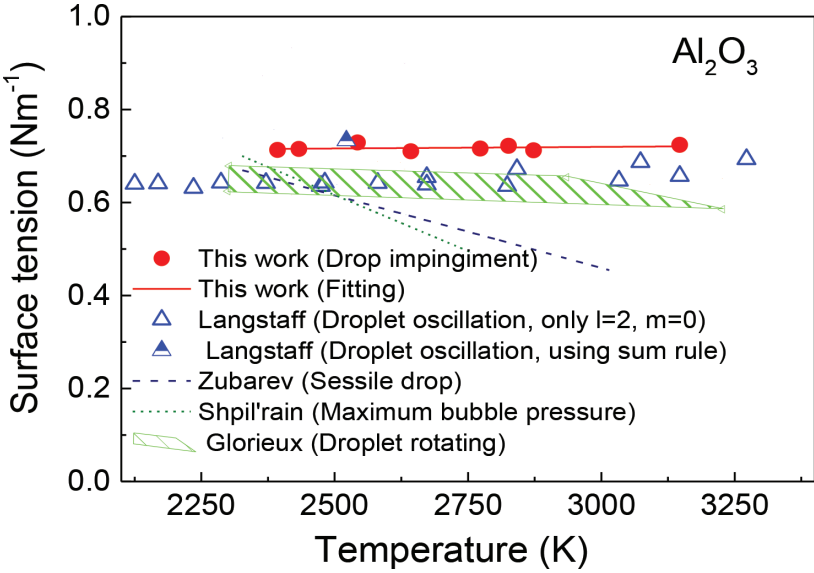


FIGURE 6
Surface tension of liquid Al_2O_3 .

(only $l = 2, m = 0$) and droplet rotating techniques. Through linear fitting, the temperature-dependent surface tension of Al_2O_3 is expressed as

$$\gamma = (0.69 \pm 1.04) \times 10^{-5} \times T + (0.70 \pm 0.03) \quad (2393 \text{ K} \leq T \leq 3147 \text{ K}). \quad (9)$$

Using Eq. (9), the surface tension of liquid Al_2O_3 at its melting temperature (2345 K) was calculated to be $0.72 \pm 0.05 \text{ N/m}$.

3.2 Uncertainty of measurements

The uncertainty of this technique arises from the process for calculating the initial kinetic energy E_k , temperature T , surface areas S_i and S_a , and energy lost through viscous deformation, E_v . E_k was determined from two adjacent images by calculating the distance moved by the center of gravity. The position of the center of gravity was determined from the sample image; therefore, ambiguous edges would result in inaccurate positioning of the center of gravity. The resultant uncertainty is expected to have a random distribution. As the deviation of our measured data shown in Fig. 6 is not significant, we inferred that the uncertainty associated with E_v was small owing to the high frame rate of the camera (2000 fps).

The temperature of the sample was estimated from the cooling curve obtained before the impingement experiment, the falling time of the sample calculated from the speed of the sample just before impingement, and the

distance between the initial sample position and the plate. The main uncertainty in this process originated from the assumption that the cooling rate of the falling sample is identical to that of the levitated sample. The cooling of the melted Al_2O_3 is influenced by two factors: heat radiation and heat transfer to the surrounding gas. As the gas flow rate around the sample was higher for the levitated sample than the dropping one, the levitated sample lost more heat through heat transfer to the surrounding gas; this means the cooling curve shown in Fig. 5 underestimates the actual sample temperature.

The actual temperature of the falling sample is expected to be between that determined using the cooling curve of the levitated sample and that calculated considering only the radiation heat loss using the Stefan–Boltzmann law [17]. Figure 7 shows the difference in the experimental cooling curve drawn for the levitated sample and that drawn using the Stefan–Boltzmann law considering the emissivity of Al_2O_3 to be 0.93 [18]. The time taken by the sample to fall on the plate was 100 ms at the most. Thus, the difference between the two cooling curves was approximately 30 K. This result indicates that our method underestimated the temperature by several tens of Kelvins. However, this underestimation does not affect the measured surface tension of Al_2O_3 significantly as the surface tension has a very weak temperature dependency; it should be noted that the impingement technique requires attention with respect to temperature estimation.

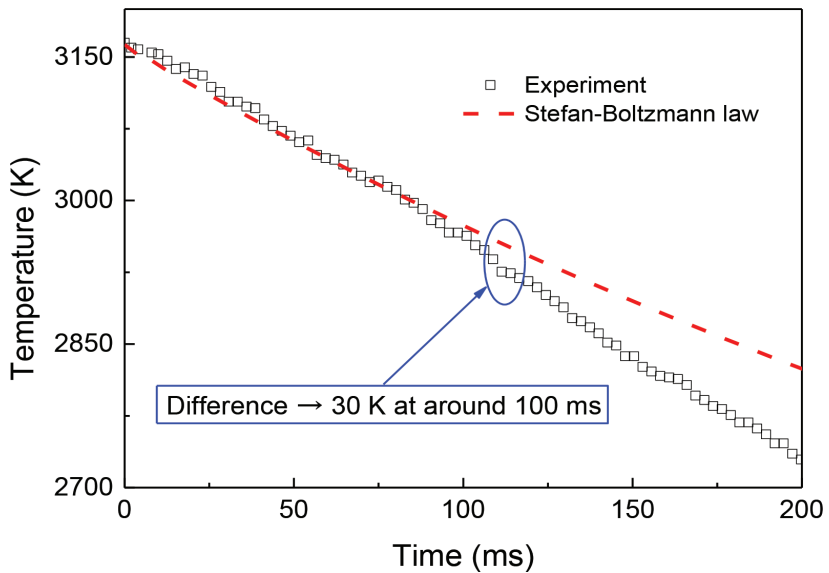


FIGURE 7
Cooling curve obtained experimentally and via calculations.

As for the evaluation of the surface area, several factors could cause uncertainty. First, we assumed that the shape of the sample before impingement was a true sphere; however, the actual shape of the sample was slightly distorted, which resulted in the underestimation of the difference in the surface area and overestimation of the resultant surface tension. Thus, the edge of the sample before impingement was fitted using an ellipsoid (Fig. 8); the ratio of the short axis to the long axis was found to be 0.995, resulting in a 1 % underestimation of the surface tension. The surface area of the deformed sample, S_d , should be evaluated when the velocity becomes zero. Otherwise, the initial kinetic energy is not fully converted to the surface energy, which leads to underestimation of the difference in the surface area and overestimation of the surface tension.

The other factors that will affect the measurements are the reaction between the sample and substrate, excessive deformation, and fragmentation of the sample. Equation (3) holds only when there is no reaction between the sample and the substrate. If the sample recoils after impingement as shown in Fig. 3(a), i.e. if it does not wet the substrate, it can be judged that the sample does not react with the substrate. If the deformation is excessive and the center of the drop is recessed, the surface tension will be considerably overestimated because the surface area of the recessed part is ignored. Fragmentation changes the mass of the sample, leading to underestimation of the initial kinetic energy and surface tension. These influence of these factors must be excluded by carefully examining the recorded images.

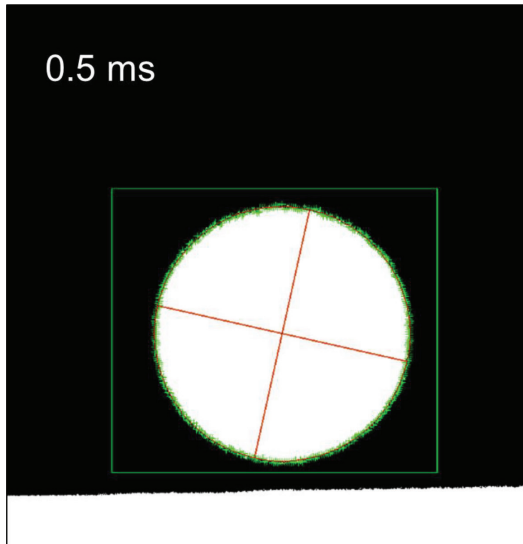


FIGURE 8
Ellipse fitting of the droplet before impingement.

4 CONCLUSIONS

In the present work, a new technique to measure the surface tension of liquid oxide melts from their impingement behavior was developed. The surface tension of molten Al_2O_3 measured using this method was approximately 0.72 N/m around its melting temperature; this value was close to that measured via the oscillation droplet method using the sum rule. The droplet impingement method can effectively measure the surface tension despite some deviations in this measurement. This method can measure the surface tension of liquids in shorter durations (approximately 80 ms) than conventional methods. Thus, it is expected that the surface tension of molten materials with high vapor pressures such as ZrO_2 and UO_2 can be measured using this method.

ACKNOWLEDGEMENT

This study is the result of “Development of viscosity and surface tension measurement technique for molten core materials” carried out under the Strategic Promotion Program for Basic Nuclear Research by the Ministry of Education, Culture, Sports, Science and Technology of Japan, “Deepening Understanding of Ex-Vessel Corium Behavior by Multi-Physics Modeling” carried out under the Strategic Promotion Program for Basic Nuclear Research by the Ministry of Education, Culture, Sports, Science and Technology of Japan (representation researcher: A. Yamaji in Waseda university), and a Grant-in-Aid for JSPS Fellows, 18J10057. We would like to thank A. Yamaji in Waseda University for useful discussions. We also thank M. Furuya in Waseda University for providing important information to improve our experiment.

REFERENCES

- [1] Wuchina, I.T.E., Opila, E., Opeka, M., Fahrenholtz, W. “UHTCs : Ultra-High Temperature Ceramic Materials for Extreme Environment Applications,” *Electrochem. Soc. Interface*, **16** (4), (2007), 30.
- [2] Fahrenholtz, W.G., Wuchina, E.J., Lee, W.E. *Ultra-High Temperature Ceramics: Materials for Extreme Environment Applications*. Hooboken: Wiley, 2014.
- [3] Hofmann, P. *Nuclear Mater.* **270** (1999), 194, [https://doi.org/10.1016/S0022-3115\(98\)00899-X](https://doi.org/10.1016/S0022-3115(98)00899-X).
- [4] Langstaff, D., Gunn, M., Greaves, G.N., Marsing, A., Kargl, F. *Rev. Sci. Instrum.*, **84** (2013), 124901, <https://doi.org/10.1063/1.4832115>.
- [5] Kondo, T., Muta, H., Kurosaki, K., Kargl, F., Yamaji, A., Furuya, M., Ohishi, Y. *Heliyon*, vol. 5, no. July, p. e02049, 2019. <https://doi.org/10.1016/j.heliyon.2019.e02049>.
- [6] Zubarev, Y.V., Kostikov, V.I., Mitin, B.S., Nagibin, Y.A., Nischeta, V.V. “Certain Properties of Molten (Liquid) Aluminum Oxide,” *Izv. Akad. Nauk SSSR Neorg. Mat.*, **5** (1968), 1563.
- [7] Shpil’rain, E.E., Yakimovich, K.A., Tsitsarkin, A.F. “Experimental Study of the Density of Liquid Alumina up to 2750 °C.,” *High Temp. Press.*, **5** (1973), 191, 1973.

- [8] Iida T., Guthrie, R.T.L. *The Physical Properties of Liquid Metals*. Oxford: Clarendon Press, 1988, <https://lib.ugent.be/catalog/rug01:000311319>.
- [9] Cummings D.L., Blackburn, D.A. *J. Fluid Mech.*, **224** (1991), 395, [10.1017/S0022112091001817](https://doi.org/10.1017/S0022112091001817).
- [10] "FactSage." [Online]. Available: www.factsage.com.
- [11] Nii, K. "Surface tension and surface stress," *Japan Inst. Met.*, **13** (1974), 321.
- [12] Goodman A.W., Goodman, G. "Generalizations of the Theorems of Pappus," *Am. Math. Mon.*, **76** (1969), 355, [doi:10.2307/2316426](https://doi.org/10.2307/2316426).
- [13] William Thomson, *Theory of Vibration with Applications*, 4th edition. Upper Saddle River, NJ, United States: Pearson Education, 1996.
- [14] Brillo, J. *Thermophysical Properties of Multicomponent Liquid Alloys*. Köln: De Gruyter Oldenbourg, 2016.
- [15] Gale, W.F., Totemeier, T.C. *Smithells Metals Reference Book*, 8th edition. Netherland: Elsevier Inc., 2004.
- [16] Glorieux, B., Millot, F., Rifflet, J.C. *Int. J. Thermophys.*, **23** (2002), 1249, <https://doi.org/10.1023/A:1019848405502>.
- [17] Boltzmann, L. *Ann. der Phys. und Chemie*, **258** (1884), 291, <https://doi.org/10.1002/andp.18842580616>.
- [18] Sarou-Kanian, V., Rifflet J.C., Millot, F. *Int. J. Thermophys.*, **26** (2005), 1263, <https://doi.org/10.1007/s10765-005-6725-5>.